Removal of crystal violet, an emerging pollutant from aqueous solution using biochar prepared from coconut shell

Jonty Rodrigues, Sugandha Shetye*, Sheba Raju

Department of Chemistry, K J Somaiya College of Science and Commerce, Vidyavihar, Mumbai 400077, India

Email: *sugandha@somaiya.edu

Received: 23.3.2024, Revised: 26.4.2024, Accepted: 27.4.2024

Abstract

Crystal violet is an emerging pollutant which may be transferred into water bodies and does not have any established guidelines for detection. Biochar, a material derived from the partial pyrolysis of biomass, exhibits remarkable potential in removing organic contaminants like crystal violet due to its porous structure. In this study coconut shell powder was subjected to pyrolysis at four distinct temperatures to obtain biochar samples. Proximate analysis was performed for all the biochar samples obtained. The sample were characterised using FTIR, SEM and XRD. Kinetics and isotherm studies were performed on the biochar to determine the mechanism of adsorption and maximum removal capacity. As the pyrolysis temperature increased the pH and ash content increased, the yield of biochar decreased. The biochar prepared at 700 °C showed the best adsorption capacity among all the prepared biochar samples. Response surface methodology suggested the optimum dosage of biochar required is 210 mg at a concentration of 12 ppm. The adsorption process adhered to second-order kinetics, and the maximum adsorption capacity, according to the Langmuir adsorption isotherm, was determined to be 124.5 $mg.g^{-1}$.

Key words: Coconut shell Biochar, Emerging Contaminants, Adsorption Studies, crystal violet, Response Surface Methodology.

Introduction

In recent years, water resources have become increasingly polluted due to overexploitation and rapid industrialization. Dyes are one of the major constituents of industrial pollutant[1]. As such a considerable effluent enters the environment and pollutes the environment, as well as enters the food chain leading to biomagnification[2]. Crystal violet is a purple-coloured dye used chiefly in textile industries for colouring cotton and silk. It is also used as a biological staining, external skin disinfectants[3], as well as an antimicrobial agent to prevent fungal growth in poultry litter[4]. The dye is potentially carcinogenic, genotoxic and mutagenic

causing development of tumour in some species of fish if persistent in environment for long periods of time[5]. It is found to be a moderate eye irritant, and can cause permanent injury to cornea and conjunctiva, and in extreme cases lead to kidney or respiratory failure[5]. Norman List of emerging pollutants[6] has included crystal violet as an emerging pollutant that is currently not included in routine monitoring programmes at the European level and which may require future regulation, depending on further research on their ecotoxicity, potential health hazards.

Many techniques have been developed for the removal of dyes from wastewater[7] such as photodegradation[8,9], chemical oxidation[10] and adsorption[11,12]. Among them adsorption techniques have been identified as cheap and efficient treatment of wastewater at scale without the use of any harmful chemical or production of side products[13].

Biochar is a carbonaceous material prepared by the pyrolysis of biomass in limited supply of oxygen[14]. The properties of biochar heavily depend on the biomass, the resident time, resident temperature, heating rate as well as chemical or physical modification to the surface[15–20]. The properties of biochar can be modified by proper control of each parameter, and it can be used for various applications[13,21,22].

Biochar has been successfully used for the removal of organic as well as inorganic contaminants[11,12,23,24]. It has been used for the removal of dyes such as methylene blue[25], Congo red[26]. Several studies have been done for the removal of crystal violet using biochar prepared using palm petioles[27], kernel shell[28], coconut husk[29], walnut shell[30], Gliricidia sepium[31], banana stem[32] and sugarcane bagasse[33]. Coconut shell is an agricultural waste which is low cost, readily available biomass[34,35]. Biochar made from coconut shell has been used for the removal of dyes such as methylene blue[36,37], Reactive Orange 16[38], Basic Red 09[39]. Most of these biomaterials exhibit varying adsorption capacities, making them valuable tools for treating dye-contaminated wastewater. Researchers continue to explore their potential and optimize their performance for sustainable environmental solutions.

As research lacks on the adsorption of crystal violet onto coconut shell biochar our objective is to prepare biochar from coconut shell at different temperatures and investigate its potential for removal of crystal violet from its aqueous solution. The factors such as resident temperature, concentration, dosage was optimized, for adsorption isotherm and kinetics studies.

Experimental

Materials: Coconut shell was procured from local market, dried in sunlight for one week and ground to a powder in a domestic mixer grinder, followed by screening through a one mm

mesh. Crystal violet (C.I. No = 42555) was procured from SD fine Chem limited India. A 500 ug/ml stock solution was prepared by dissolving 500 mg of crystal violet in 1000 mL of distilled water.

Biochar Preparation: Powdered coconut shell was pyrolyzed in a steel container at four different temperatures, 400 °C, 500 °C, 600 °C, 700 °C for half an hour. Three samples of biochar at each temperature were prepared and stored separately. The percentage yield of the biochar was calculated using Eq. (1) [40]:

$$\%Yield = \frac{m_{bc}}{m_{bm}} \times 100 \ \#(1)$$

Where, m_{bc} is the weight of the biochar and m_{bm} is the weight of the biomass before pyrolysis.

Proximate Analysis: For pH determination, biochar was mixed with distilled water in a ratio of 1:20 and kept for 24 hours after which the pH was measured[41]. For Ash Content ASTM D3174 was used [41,42].

Characterization : To determine the functional groups on the biochar samples, FTIR of all the four biochar samples was done. Further, SEM and XRD analysis of biochar having the maximum adsorption capacity was carried out.

Adsorption Studies: Batch adsorption studies were carried out to determine the amount of crystal violet adsorbed onto the biochar. After each adsorption study the solution was filtered through a Whatmann filter paper no 41, followed by measuring the absorption of the solution on a JASCO V-620 UV-Vis spectrometer at 590 nm. A linear calibration curve was used to determine the concentration of the crystal violet in the solution. The percentage removal was calculated using Eq. (2) [43]:

$$\%Removal = \frac{(C_i - C_t)}{(C_i)} \times 100 \ \#(2)$$

Where, C_t Is the final concentration, C_i is the initial concentration.

Adsorption capacity was calculated using Eq. (3) [43]:

$$\mathrm{Q} = \frac{x}{M} \ \#(3)$$

Where, Q represents the adsorption capacity in $mg.g^{-1}$. x represents the mass of the adsorbate adsorbed in mg. M represents the mass in grams of the biochar.

Performance evaluation of biochar samples: To evaluate the performance of each biochar sample, adsorption capacity of each sample was determined. 250 mg of each biochar sample

was shaken on an orbital shaker for 2 hours with 100 mL of 10 ppm crystal violet solution in a 250 mL conical flask. This process was done in triplicate.

Optimization of parameters: Response surface methodology (RSM), a multivariate statistical technique was used for optimization of the two parameters, concentration of the dye and dosage of biochar[44,45]. A central composite design (CCD) was used to decide the number of experiments. Ten experiments were performed with the adsorption capacity and percentage removal as two response variables.

Adsorption Kinetics and Isotherm: To determine the mechanism and kinetics of the adsorption, the study was performed in two steps:

Isotherm Fitting: 250 mg of biochar was added in eight different conical flasks. To each flask 100 ml of 1, 5, 10, 20, 50 100, 250, 500 ppm of crystal violet was added and shaken on an orbital shaker for 2 hours, the results obtained from this experiment was used to perform the isotherm fitting.

Kinetic Experiment: 250 mg of biochar was added in seven different conical flasks. To each flask 100 ml of 10 ppm crystal violet solution was added. All the flasks were shaken on an orbital shaker for 2, 5, 10, 20, 40, 70 and 100 min. The solution was filtered through a Whatman filter paper no 41, followed by measuring the absorbance of the solution on a JASCO V-620 UV-Vis spectrometer at 590 nm.

Statistical Analysis and Model Fitting: Analysis of Variance (ANOVA) was performed using Minitab 21, with $p < 0.05$ signifying statistical significance. Response Surface Methodology was performed using Design Expert 13 and model fitting was performed using Origin Pro 2021.

Result and Discussion

Biochar Preparation: The results from the yield are given in Table 1. The difference in yields of biochar produced at different temperatures showed a statistically significant difference ($p < 0.05$). Each pair, student's t-test showed that, there was a statistically significant difference in the yields of biochar except that produced at 600 °C and 700 °C (Fig. 1). There is a decrease in yield with an increase in temperature of pyrolysis. The decrease in yield could be attributed to decomposition of lignin, which occurs at a higher temperature than that of hemicellulose, enhancing properties such as surface area and pore size[46,47]. Furthermore, no appreciable change in yield was observed beyond 600 °C. At temperatures about 550 °C the fixed carbon reaches a steady state and there is little to no decrease in yield[48].

Proximate Analysis: The pH and ash content (Table 1) of all the biochar samples were statistically different from each other ($p > 0.05$), suggesting that there is a change in ash content and pH as the pyrolysis temperature changes. It is observed that with an increase in pyrolysis temperature the ash content of biochar is increasing, which may be attributed to the increased concentration of inorganic matter after volatilization of organic matter[40]. A similar trend can be seen in pH, as the temperature increases the pH of the biochar increases. This could be attributed to the increase in alkaline salts and reduction of acidic functional groups[19,49].

Characterization: Biochar like other agricultural biomass is typically made up of cellulose, hemicellulose and lignin[50]. Fig. 3 shows the FTIR spectra of CS400, CS500, CS600 and CS700 biochar. A considerable broad O-H stretching at around 3384 cm^{-1}, a prominent C-H stretching at 2950 cm^{-1}, aromatic C=O and C=C was observed at about 1698 cm^{-1} [44]. A C-O-C lignin stretching was observed at 1243 cm^{-1} [40] and a C-O-C cellulose/hemicellulose (holocellulose) stretching was observed at 1049 cm^{-1} [40]. A peak at 870 cm^{-1} corresponds to O-Si stretching, due to presence of silicates in biochar[51]. It is observed that as the temperature increases, there was a reduction in oxygen containing functional groups. This is due the thermal decomposition of lignin, cellulose and hemicellulose[52]. A relative increase of silicate functional group was also observed, this could be attributed to the ash present in the biochar and high thermal stability of silicates in biochar.

As CS700 biochar showed the best removal capacity among all the prepared biochar, it was selected for SEM and XRD characterization. Fig. 4 shows the Scanning Electron Microscopy (SEM) images of CS700 before and after adsorption of crystal violet. At a magnification of 5k the smooth, well organised, porous, carbonaceous cellular framework of coconut shell can be clearly seen[43]. Comparison of images before and after adsorption suggest the deposition of crystal violet on the biochar and the available pores were fully occupied.

The X-ray diffraction (XRD) pattern was collected on an X-ray diffraction (XRD) spectroscopy with Cu Kα radiation (λ = 1.5405 Å) over the angular range $10° \leq 2\theta \leq 70°$, operating at 40 kV and 30 mA. Fig. 5 shows the XRD patterns of biochar before and after adsorption of crystal violet. A broad low intensity peak at about 23° was observed, which could be due to the presence of crystalline carbon present in the structure, mostly cellulose[53]. This is in good agreement with the XRD pattern reported previously[54]. The XRD pattern confirms that the prepared biochar was mostly amorphous in nature[54].

Performance evaluation of biochar samples: As seen in Fig. 6 increase in the pyrolysis temperature increased the adsorption capacity, gradually with temperature. The biochar

prepared at 700 °C showed the highest average adsorption capacity with the lowest standard deviation. The increase in adsorption could be attributed to the increased surface area, high porosity and surface morphological changes[19,55]. Therefore, the biochar prepared at 700 °C was selected to perform further studies.

Response Surface Methodology: According to the given design (Table 2), ten experimental runs were conducted.

The results were then analysed using the analysis control and a summary of fit of all the models are given in Table 3. In case of the adsorption capacity, a linear model was suggested with a sequential p-value of 0.0011 and Adjusted R^2 to 0.8152. Thus, this model was selected for further analysis. For the removal capacity, both the linear and quadratic models were suggested but as the adjusted R^2 of the quadratic model was higher the quadratic model was selected whereas the terms in the cubic models were aliased due to low factor count, they were ignored.

The equations for the adsorption capacity (Y_1) and Percentage Removal (Y_2) are given as Eq. (4) and Eq. (5):

$$Y_1 = 5.9964 - 0.0155\,X_1 + 0.14513\,X_2 \;\#(4)\#\#\#\#\#\#\#$$

$$Y_2 = 66.5279 + 0.0438\,X_1 - 2.3224\,X_2 + 0.00237\,X_1X_2 - 0.00012\,{X_1}^2 + 0.02002\,{X_2}^2 \;\#\#(5)$$

The selected models were then used for numerical optimization, with the default options and a dosage value of 210 mg and concentration of 12 ppm was obtained, with an overall desirability of 0.693, the contour plots of all the factors are given in Fig. 7.

Adsorption Isotherms: A non-linear Langmuir and Freundlich isotherms were fitted, to understand the mechanisms of adsorption of the crystal violet onto the surface of biochar.

The Langmuir adsorption isotherm assumes that the adsorption occurs on a monolayer, and once the sites have been occupied no further adsorption occurs [4].

The Freundlich isotherm assumes that the adsorption occurs on heterogeneous surface[4].

The Langmuir equation is given as Eq. (6) [4,56]:

$$Q_e = \frac{K_a Q_{max} C_e}{1 + K_a C_e} \;\#(6)$$

And the Freundlich isotherm is given as Eq. (7) [4,56]:

$$Q_e = {K_f C_e}^{1/n} \;\#(7)$$

Where, K_a is the Langmuir isotherm constant and Q_{max} (mg.g^{-1}) is the maximum adsorption capacity. Q_e (mg.g^{-1}) is the amount of adsorbate on the surface of the adsorbent at equilibrium and C_e is the concentration of the solution (mg.L^{-1}). K_f is the Freundlich isotherm constant, and n (Freundlich exponent) is an indicator of intensity change during adsorption process. The results of the fits are given in table .

As the Freundlich model showed a better fit (R^2=0.99) this indicates that a multilayer adsorption process, and the adsorption occurs on heterogeneous sites[43], this is similar to previous work[4,29,43]. The maximum adsorption capacity calculated from the Langmuir adsorption isotherm of 124.5 mg.g^{-1} showed an excellent removal capacity for crystal violet.

Adsorption Kinetics: The results from kinetics experiments were used to fit, a non-linear Pseudo-first-order (PFO) and Pseudo-second-order (PSO) kinetics modes, to understand the rate and the order of the reaction. The PFO model equation is given as Eq. (8)[57]:

$$Q_t = Q_e\left(1 - e^{(-k_1 \times t)}\right) \#(8)$$

The PSO model equation is given as Eq. (9)[57]:

$$Q_t = \frac{{Q_e}^2 k_2 t}{1 + {Q_e}^2 k_2 t} \#(9)$$

Where Q_e and Q_t (mg.g^{-1}) are adsorption capacity at equilibrium and t time (h), respectively, k_1 (min^{-1}) and k_2 (g.mg^{-1}·min^{-1}) are the constants for pseudo-first and pseudo-second order models, respectively. The results of the fitting paraments are given in Table .

The PSO model was a good fit for the adsorption of crystal violet onto the surface of biochar showing that the adsorption follows a second order kinetics process with a rate constant of 0.24153 (g.mg^{-1}·min^{-1}). As seen in Fig. 9 90 % adsorption occurred during the first few minutes of the adsorption process showing that the adsorption process is a kinetically favourable process[58]. The PSO model confirms chemisorption as the rate-limiting step caused by the involvement of physicochemical interactions between the two phases[59]. This is in agreement with previous studies[4,29,43].

Comparison of biochar: A summary of various biomass materials used to prepare biochar for the removal of dyes from aqueous solutions is given in Table 6. Biochar prepared from coconut shell has a moderate adsorption capacity as compared to other types of biochar. Modification of biochar properties is possible with techniques such as chemical and physical modification[18,36], but this adds further cost and complexity for preparation of biochar from a relatively low-cost biomass[60].

Conclusion

Biochar prepared from coconut shell powder was tested for it's potential for removal of crystal violet from simulated water samples. Biochar prepared at a temperature of 700 °C showed the best adsorption capacity among all the prepared biochar for crystal violet. The results from the FTIR analysis showed that as the temperature increased, the oxygen functional group decreased. SEM analysis showed that the prepared biochar had a well-organized porous structure. The XRD pattern showed that the biochar was mostly amorphous in nature, with no crystalline inorganic contaminant. The crystal violet mostly adsorbed into the mesoporous structures of the biochar. Optimization of dosage and concentration was performed using CCD and yielded a dosage of 210 mg and 12 ppm, with desirability of 0.693. The results from the optimization can be for future studies using crystal violet and coconut shell biochar. The maximum removal capacity Q_{max} was found to be 124.5 $mg.g^{-1}$ and the adsorption followed a second order kinetic with a rate constant of 0.241 $g.mg^{-1}\cdot min^{-1}$. Thus, biochar prepared from coconut shell can be used as a low cost, sustainable solution for removal of emerging pollutants such as crystal violet and other dyes.

Acknowledgements and funding statements

Acknowledgements: The author would like to thank Dr Abhay Sinh Salunke for his continuous help and support during the preparation of this work. The authors would also like to thank

Dr P A Hassan, BARC for providing support for this project.

Figures:

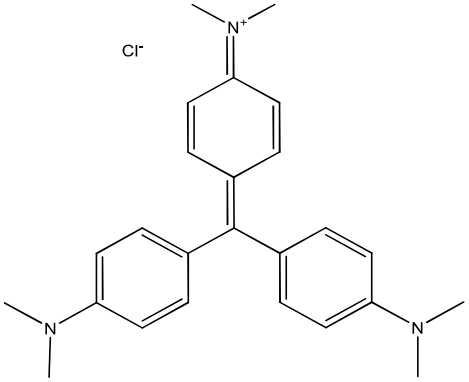

Fig. 1: Structure of crystal violet.

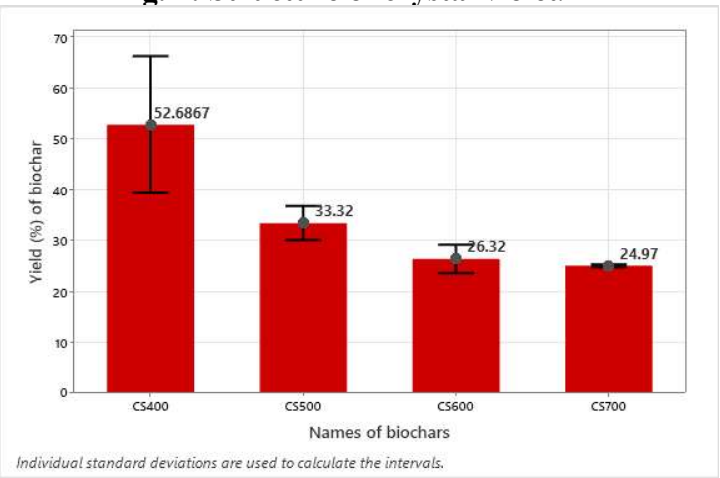

Fig. 2: Bar graph showing the yield of biochar at various temperature.

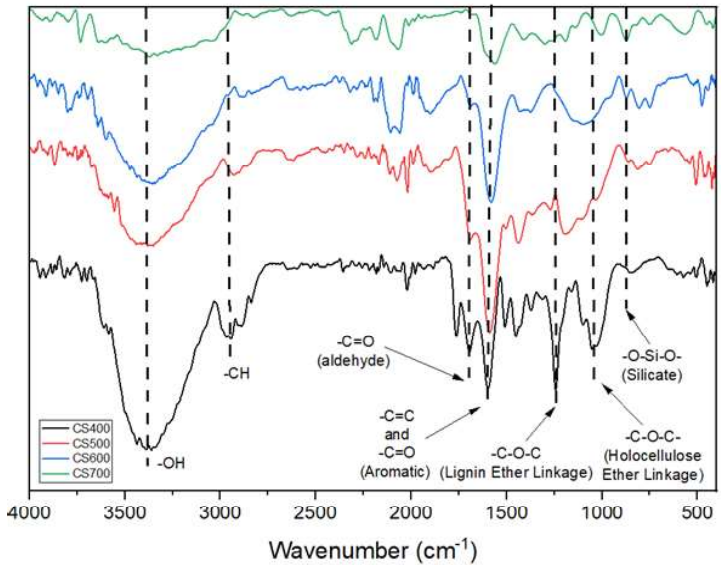

Fig. 3: FTIR spectra of CS400, CS500, CS600, CS700

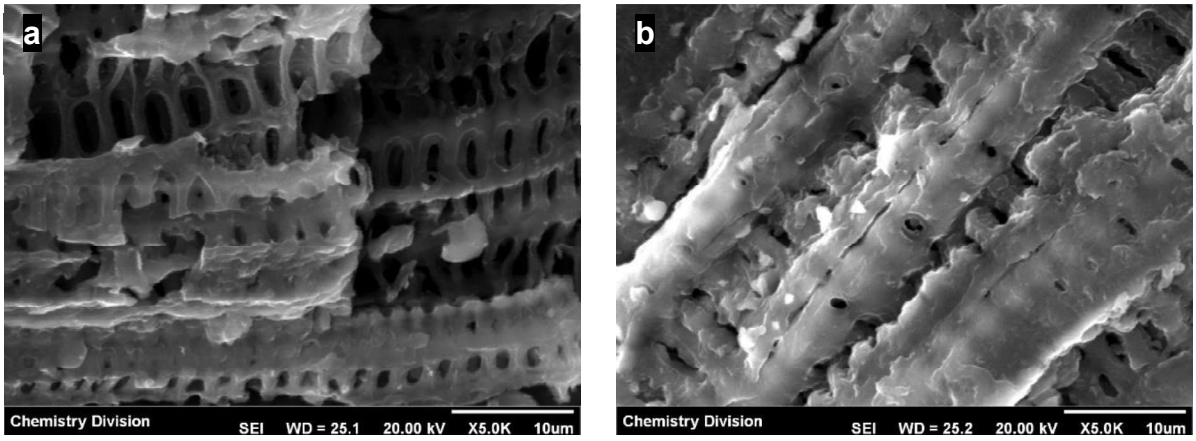

Fig. 4: SEM images of CS700 (a) before and (b) after adsorption.

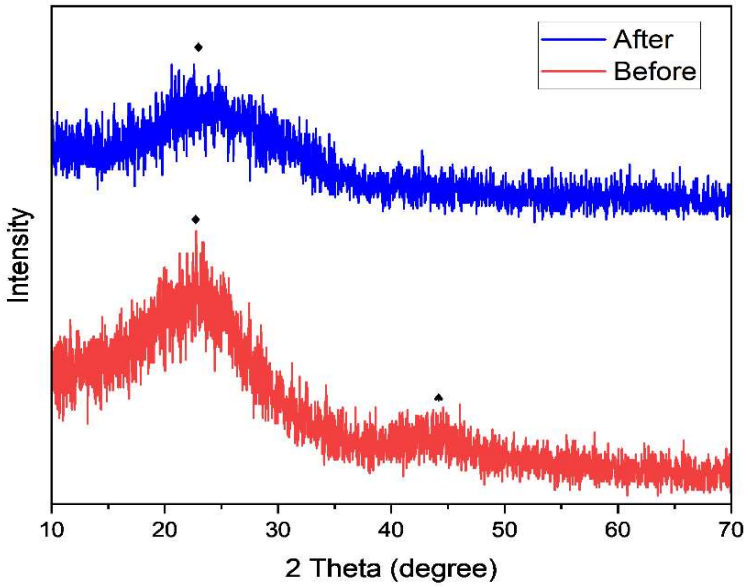

Fig. 5: XRD pattern of CS700 before and after adsorption.

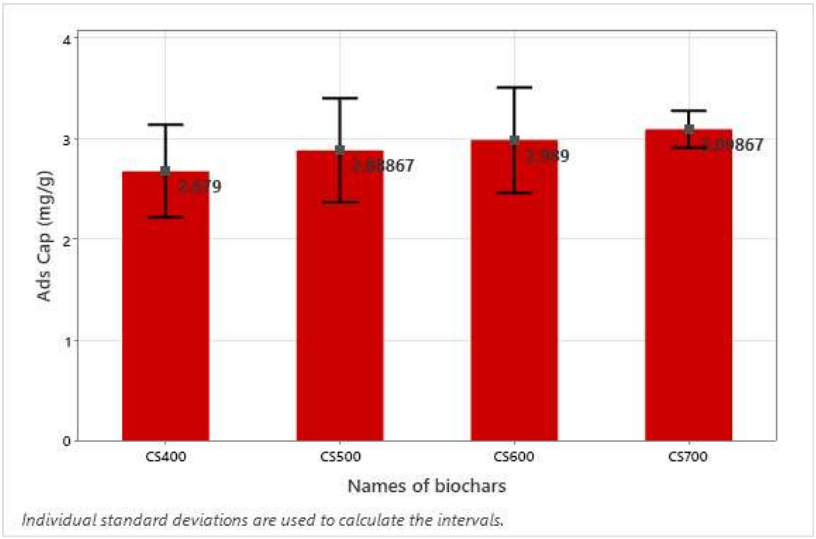

Fig. 6 : Plots of Adsorption Capacity of CS400, CS500, CS600, CS700.

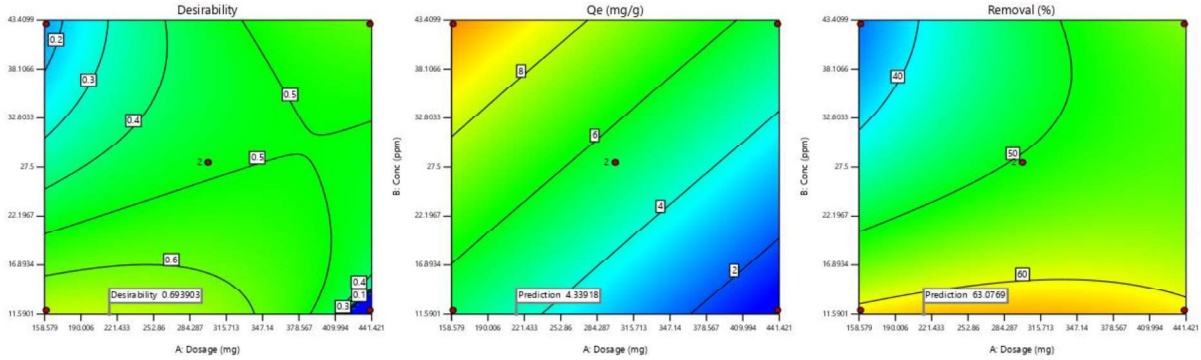

Fig.7: Contour Plot of Optimized results.

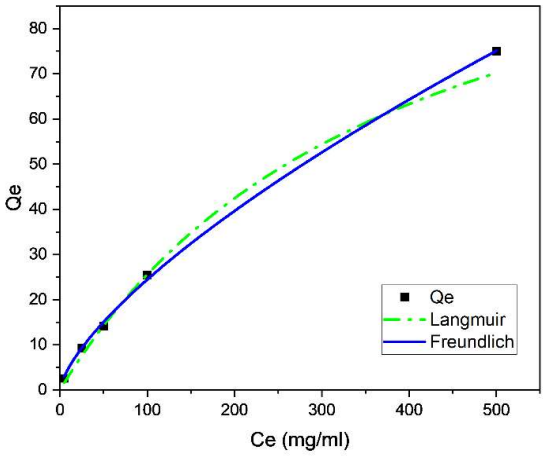

Fig. 8: Adsorption isotherms of crystal violet.

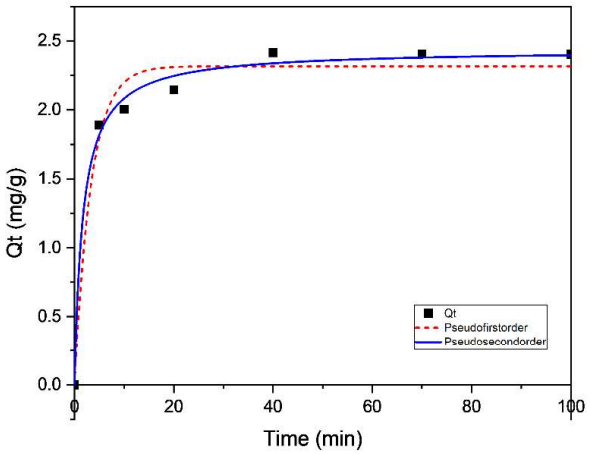

Fig. 9: Adsorption kinetics of crystal violet onto biochar.

Tables:

Table 1: The yield, Ash Content and pH of biochar derived from coconut shell, at four pyrolysis temperatures ranging from 400 °C to 600 °C.

Label	Percentage Yield	Ash Content	pH
CS400	52.68±5.41[a]	1.58±0.02[a]	7.68±0.16[a]
CS500	33.32±1.35[b]	1.88±0.04[b]	8.01±0.13[b]
CS600	26.32±1.12[c]	2.23±0.02[c]	8.31±0.05[c]
CS700	24.97±0.10[c]	2.82±0.00[d]	8.77±0.01[d]

Mean ± Standard deviation; The different letters following the figures indicate significant differences ($p < 0.05$).

Table 2: Experimental Design and Variables of CCD

Std Order	Run Order	X1	X2	Qe ($mg.g^{-1}$)	Removal (%)
8	1	300	50	9.21091	55.2654
7	2	300	5	1.1784	70.704
5	3	100	28	11.1173	39.7045
10	4	300	28	4.90239	52.5256
9	5	300	28	4.54942	48.7438
6	6	500	28	3.13807	56.037
3	7	160	43	8.15145	30.331
1	8	160	12	4.64264	61.9019
4	9	440	43	4.9118	50.2603
2	10	440	12	1.67117	61.2763

Table 3: Summary of fits of Linear, 2 factor interaction, quadratic and cubic models for (a) Adsorption capacity and (b) Percentage removal.

(a) Fits summary of Adsorption Capacity					
Source	**Sequential p-value**	**Lack of Fit p-value**	**Adjusted R^2**	**Predicted R^2**	
Linear	**0.0011**	**0.1273**	**0.8152**	**0.6707**	**Suggested**
2FI	0.9109	0.1155	0.7848	0.5279	
Quadratic	0.4261	0.1073	0.7893	0.3448	
Cubic	0.3879	0.0865	0.8366	-1.2978	**Aliased**
(b) Fits summary of Removal Capacity					
Source	**Sequential p-value**	**Lack of Fit p-value**	**Adjusted R^2**	**Predicted R^2**	
Linear	**0.0319**	**0.2352**	**0.5197**	**0.1281**	**Suggested**
2FI	0.2193	0.2441	0.5734	0.2109	
Quadratic	**0.0966**	**0.3280**	**0.8011**	**0.3952**	**Suggested**
Cubic	0.4583	0.2516	0.8177	-1.2455	**Aliased**

Table 4: Fitted Parameters of the Langmuir and Freundlich isotherms.

Isotherm	Parameters		R^2
Langmuir	Q_{max} ($mg.g^{-1}$)	K_a ($L.mg^{-1}$)	0.97
	124.5	0.00234	
Freundlich	K_f	n	0.99
	0.9308	1.40955	

Table 5: Kinetics Model parameters of PFO and PSO kinetics model

Model	Parameters		R^2
PFO	Q_e ($mg.g^{-1}$)	k_1 (min^{-1})	0.97
	2.31631	0.29808	
PSO	Q_e ($mg.g^{-1}$)	k_2 ($g.mg^{-1}\cdot min^{-1}$)	0.99
	2.43695	0.24153	

Table 6: Comparison of various biochar in literature

Biomass	Adsorbate	Maximum Adsorption Capacity ($mg.g^{-1}$)	Ref
Palm petioles	Crystal violet	209	[27]
Gliricidia sepium		125.53	[31]
Palm Kernal Shell		25.45	[28]
Banana Stem		153.50	[32]
Coconut Shell	Methylene Blue	200.01	[36]
		8.612	[37]
	Reactive Orange 16	106.60	[38]
	Basic Red 09	65.24	[39]
Coconut Shell	Crystal violet	124.5	this study

References

1. R. Al-Tohamy, S. S. Ali, F. Li, K. M. Okasha, Y. A. G. Mahmoud, T. Elsamahy, H. Jiao, Y. Fu, and J. Sun,*Ecotoxicol Environ Saf*, 231, 113160, 2022.
2. B. Lellis, C. Z. Fávaro-Polonio, J. A. Pamphile, and J. C. Polonio,*Biotechnology Research and Innovation*, 3, 275, 2019.
3. M. Saji, S. Taguchi, K. Uchiyama, E. Osono, N. Hayama, and H. Ohkuni,*J Hosp Infect*, 31, 225, 1995.
4. A. Mittal, J. Mittal, A. Malviya, D. Kaur, and V. K. Gupta,*J Colloid Interface Sci*, 343, 463, 2010.
5. S. Mani and R. N. Bharagava,*Rev Environ Contam Toxicol*, 237, 71, 2016.
6. https://www.norman-network.net/?q=node/19 accessed: 22-04-2024
7. M. T. Amin, A. A. Alazba, and U. Manzoor,*Advances in Materials Science and Engineering*, 2014, 1, 2014.
8. N. Welter, J. Leichtweis, S. Silvestri, P. I. Z. Sánchez, A. C. C. Mejía, and E. Carissimi,*J Alloys Compd*, 901, 163758, 2022.
9. N. P. F. Gonçalves, M. A. O. Lourenço, S. R. Baleuri, S. Bianco, P. Jagdale, and P. Calza,*J Environ Chem Eng*, 10, 107256, 2022.
10. X. Li, Y. Jia, M. Zhou, X. Su, and J. Sun,*J Hazard Mater*, 397, 122764, 2020.
11. R. Guo, L. Yan, P. Rao, R. Wang, and X. Guo,*Environmental Pollution*, 258 2020.
12. E. Baldikova, K. Pospiskova, and I. Safarik,*Chem Eng Technol*, 43, 168, 2020.
13. F. L. Braghiroli, H. Bouafif, C. M. Neculita, and A. Koubaa,*Water Air Soil Pollut*, 229 2018.
14. X. Tan, Y. Liu, G. Zeng, X. Wang, X. Hu, Y. Gu, and Z. Yang,*Chemosphere*, 125, 70, 2015.
15. J. A. Ippolito, L. Cui, C. Kammann, N. Wrage-Mönnig, J. M. Estavillo, T. Fuertes-Mendizabal, M. L. Cayuela, G. Sigua, J. Novak, K. Spokas, and N. Borchard,*Biochar*, 2, 421, 2020.
16. E. Thomas, N. Borchard, C. Sarmiento, R. Atkinson, and B. Ladd,*Biochar*, 2, 151, 2020.

17. J. S. Cha, S. H. Park, S.-C. Jung, C. Ryu, J.-K. Jeon, M.-C. Shin, and Y.-K. Park,*Journal of Industrial and Engineering Chemistry*, 40, 1, 2016.

18. L. Wang, Y. S. Ok, D. C. W. Tsang, D. S. Alessi, J. Rinklebe, O. Mašek, N. S. Bolan, and D. Hou,*Soil Use Manag*, 38, 14, 2022.

19. S. Li, S. Harris, A. Anandhi, and G. Chen,*J Clean Prod*, 215, 890, 2019.

20. P. R. Yaashikaa, P. S. Kumar, S. Varjani, and A. Saravanan,*Biotechnology Reports*, 28, e00570, 2020.

21. C. Wang, D. Luo, X. Zhang, R. Huang, Y. Cao, G. Liu, Y. Zhang, and H. Wang,*Environmental Science and Ecotechnology*, 10, 100167, 2022.

22. M. Ahmad, A. U. Rajapaksha, J. E. Lim, M. Zhang, N. Bolan, D. Mohan, M. Vithanage, S. S. Lee, and Y. S. Ok,*Chemosphere* 99, 19, 2014.

23. Y. Yao, B. Gao, M. Inyang, A. R. Zimmerman, X. Cao, P. Pullammanappallil, and L. Yang,*J Hazard Mater*, 190, 501, 2011.

24. P. Wijeyawardana, N. Nanayakkara, C. Gunasekara, A. Karunarathna, D. Law, and B. K. Pramanik,*Environ Technol Innov*, 28 2022.

25. Y. Mu, H. Du, W. He, and H. Ma,*Diam Relat Mater*, 121, 108795, 2022.

26. S. Kaur, S. Rani, and R. K. Mahajan,*J Chem*, 2013, 1, 2013.

27. H.-O. Chahinez, O. Abdelkader, Y. Leila, and H. N. Tran,*Environ Technol Innov*, 19, 100872, 2020.

28. P. P. Kyi, J. O. Quansah, C.-G. Lee, J.-K. Moon, and S.-J. Park,*Applied Sciences*, 10, 2251, 2020.

29. A. M. Aljeboree, A. F. Alkaim, and A. H. Al-Dujaili,*Desalination Water Treat*, 53, 3656, 2015.

30. Y. Shkliarenko, V. Halysh, and A. Nesterenko,*Water (Basel)*, 15, 1536, 2023.

31. A. W. Indika and H. M. C. M. I. Meththika Vithanage,*Environ Geochem Health*, 41 2017.

32. S. K. Jadhav and S. R. Thorat,*Oriental Journal Of Chemistry*, 38, 475, 2022.

33. F. M. Jais, S. Ibrahim, C. Y. Chee, and Z. Ismail,*Sustain Chem Pharm*, 24 2021.

34. K. Harshwardhan and K. Upadhyay,*Journal of Fundamentals of Renewable Energy and Applications*, 07 2017.

35. W. L. Bradley and S. Conroy,*E3S Web of Conferences*, 130, 01034, 2019.

36. M. A. Islam, M. J. Ahmed, W. A. Khanday, M. Asif, and B. H. Hameed,*J Environ Manage*, 203, 237, 2017.

37. P. T. Le, H. T. Bui, D. N. Le, T. H. Nguyen, L. A. Pham, H. N. Nguyen, Q. S. Nguyen, T. P. Nguyen, N. T. Bich, T. T. Duong, M. Herrmann, S. Ouillon, and T. P. Q. Le,*Adsorption Science and Technology*, 2021 2021.

38. R. Muralikrishnan and C. Jodhi,*ChemistrySelect*, 5, 7734, 2020.

39. P. Saravanan, B. P. Thillainayagam, G. Ravindiran, and J. Josephraj,*Energy Sources, Part A: Recovery, Utilization, and Environmental Effects*, 2020.

40. S.-X. Zhao, N. Ta, and X.-D. Wang,*Energies (Basel)*, 10, 1293, 2017.

41. D. Angin,*Bioresour Technol*, 128, 593, 2013.

42. ASTM International,D3174 Standard Test Method for Ash in the Analysis Sample of Coal and Coke from Coal 2018.

43. J. Missau, D. A. Bertuol, and E. H. Tanabe,*Appl Clay Sci*, 214, 106297, 2021.

44. R. Zhou, M. Zhang, J. Zhou, and J. Wang,*Sci Rep*, 9 2019.

45. R. Zhou, M. Zhang, J. Li, and W. Zhao,*J Environ Chem Eng*, 8, 104198, 2020.

46. S. Li and G. Chen,*Waste Management*, 78, 198, 2018.

47. F. Amalina, A. Syukor Abd Razak, S. Krishnan, H. Sulaiman, A. W. Zularisam, and M. Nasrullah,*Cleaner Materials*, 6, 100137, 2022.

48. J. Yu, M. Song, and Z. Li,*Green Processing and Synthesis*, 11, 423, 2022.

49. A. Tomczyk, Z. Sokołowska, and P. Boguta,*Rev Environ Sci Biotechnol*, 19, 191, 2020.

50. Q. Wang and J. Sarkar,*International Journal of Energy Production and Management*, 3, 34, 2018.

51. R. Choudhary, S. Koppala, and S. Swamiappan,*Journal of Asian Ceramic Societies*, 3, 173, 2015.

52. M. Behrens, J. S. Cross, H. Akasaka, and N. Ohtake,*Biomass Bioenergy*, 122, 290, 2019.

53. D. Ciolacu, F. Ciolacu, and V. I. Popa,*Cellulose Chem. Technol*, 45, 13, 2011.

54. M. L. Yeboah, X. Li, and S. Zhou,*Materials 2020, Vol. 13, Page 625*, 13, 625, 2020.

55. S. Li, V. Barreto, R. Li, G. Chen, and Y. P. Hsieh,*J Anal Appl Pyrolysis*, 133, 136, 2018.

56. R. Zhou, Y. Wang, M. Zhang, P. X. Yu, and J. Li,*Environ Monit Assess*, 191 2019.

57. T. Chen, L. Luo, S. Deng, G. Shi, S. Zhang, Y. Zhang, O. Deng, L. Wang, J. Zhang, and L. Wei,*Bioresour Technol*, 267, 431, 2018.

58. E. D. Revellame, D. L. Fortela, W. Sharp, R. Hernandez, and M. E. Zappi,*Clean Eng Technol*, 1, 100032, 2020.

59. D. Pandey, A. Daverey, K. Dutta, V. K. Yata, and K. Arunachalam,*Environ Technol Innov*, 25, 102200, 2022.

60. T. Józwiak, U. Filipkowska, P. Bugajska, and T. Kalkowski,*Journal of Ecological Engineering*, 19, 129, 2018.